Am. J. Hum. Genet. 72:1401–1411, 2003

Disruption of the Serine/Threonine Kinase 9 Gene Causes Severe X-Linked Infantile Spasms and Mental Retardation

Vera M. Kalscheuer,[1] Jiong Tao,[1] Andrew Donnelly,[2] Georgina Hollway,[2] Eberhard Schwinger,[6] Sabine Kübart,[1] Corinna Menzel,[1] Maria Hoeltzenbein,[1] Niels Tommerup,[7] Helen Eyre,[2] Michael Harbord,[3] Eric Haan,[4,5] Grant R. Sutherland,[2,5] Hans-Hilger Ropers,[1] and Jozef Gécz[2,5]

[1]Max-Planck-Institute for Molecular Genetics, Berlin; Departments of [2]Cytogenetics and Molecular Genetics, and [3]Neurology, and [4]South Australian Clinical Genetics Service, Women's and Children's Hospital, and [5]Department of Pediatrics, The University of Adelaide, Adelaide, Australia; [6]Institute for Human Genetics Lübeck, Lübeck, Germany; and [7]Wilhelm Johannsen Centre for Functional Genome Research, Institute of Medical Biochemistry and Genetics, The Panum Institute, Copenhagen

X-linked West syndrome, also called "X-linked infantile spasms" (ISSX), is characterized by early-onset generalized seizures, hypsarrhythmia, and mental retardation. Recently, we have shown that the majority of the X-linked families with infantile spasms carry mutations in the aristaless-related homeobox gene (*ARX*), which maps to the Xp21.3-p22.1 interval, and that the clinical picture in these patients can vary from mild mental retardation to severe ISSX with additional neurological abnormalities. Here, we report a study of two severely affected female patients with apparently de novo balanced X;autosome translocations, both disrupting the serine-threonine kinase 9 (*STK9*) gene, which maps distal to *ARX* in the Xp22.3 region. We show that *STK9* is subject to X-inactivation in normal female somatic cells and is functionally absent in the two patients, because of preferential inactivation of the normal X. Disruption of the same gene in two unrelated patients who have identical phenotypes (consisting of early-onset severe infantile spasms, profound global developmental arrest, hypsarrhythmia, and severe mental retardation) strongly suggests that lack of functional STK9 protein causes severe ISSX and that *STK9* is a second X-chromosomal locus for this disorder.

Introduction

Infantile spasms are frequent, with incidence rates similar among different populations studied, ranging from 2 to 5 per 10,000 live births. Mental retardation occurs in 70%–90% of patients with infantile spasms (for review, see Wong and Trevathan 2001). Generally, the onset of infantile spasms is during the 1st year of life. Spasms tend to occur in clusters and usually involve the muscles of the neck, trunk, and extremities. Other neurological abnormalities, such as cerebral atrophy, structural malformations, and hydrocephalus, are often reported. Many of these patients have neurological impairment prior to the onset of spasms, and their intellectual prognosis is generally poor. Infantile spasms syndrome, or what is often referred to as "West syndrome" (WS), is characterized by the triad of infantile spasms (as a seizure type), hypsarrhythmia, and severe-to-profound mental retardation (Wong and Trevathan 2001). Although most cases of infantile spasms are sporadic, at least some familial cases exist and have been studied. Among these is the form of X-chromosome–linked WS, or X-linked infantile spasms (ISSX [MIM 308350]). Recently, we have identified the underlying defect in four unrelated families with ISSX (one from each of the following sources: Strømme et al. [1999], Claes et al. [1997], Bruyere et al. [1999], and our observations of one small unpublished family with ISSX) by finding mutations in the *ARX* gene, an X-linked homeobox-containing gene, which is the ortholog of the *Drosophila* aristaless-related homeobox gene (Bienvenu et al. 2002; Strømme et al. 2002*b*). Only one previously published family with ISSX (family B reported by Claes et al. [1997]) did not have a mutation in the *ARX* gene (Strømme et al. 2002*b*).

In humans, *ARX* mutations cause various forms of epilepsy, including infantile spasms, myoclonic seizures, and peripheral dystonia, as well as syndromic and nonsyndromic X-linked mental retardation (Bienvenu et al. 2002; Scheffer et al. 2002; Strømme et al. 2002*a*, 2002*b*) and lissencephaly with abnormal genitalia (Kitamura et al. 2002).

In the present study, we describe two severely affected, unrelated female patients with apparently balanced X;autosome translocations. In both patients, the

Received November 22, 2002; accepted for publication March 14, 2003; electronically published May 7, 2003.

Address for correspondence and reprints: Dr. Vera Kalscheuer, Max-Planck-Institute for Molecular Genetics, Ihnestrasse 73, D-14195 Berlin, Germany. E-mail: kalscheu@molgen.mpg.de

0002-9297/2003/7206-0005$15.00

X-chromosomal breakpoints are at Xp22.3 and are therefore distal to *ARX*, and molecular investigations have shown that both disrupt the ubiquitously expressed serine-threonine kinase 9 (*STK9*) gene. These observations, as well as functional considerations, suggest that we have identified a second locus for the X-linked WS/ISSX and thus further elucidated its genetic heterogeneity.

Subjects and Methods

Subjects

Patient 1 is the second child of healthy unrelated parents. The girl was born—after a normal pregnancy, complicated only by bleeding in the 2nd mo—10 d after term, with Apgar scores of 9 at 1 min and 10 at 5 min and with normal birth weight (3,410 g), length, and head circumference. When the patient was 3 wk old, the parents noted mild hyperexcitability, and when she was 6–8 wk, they noted abnormal turning of the eyes. Initially, motor development was normal, and electroencephalograms (EEGs) gave normal results. At the age of 3 mo, EEG showed hypsarrhythmia, and infantile spasms were diagnosed. At the age of 4.5 mo, tonic-clonic seizures became more frequent, and motor retardation and generalized hypotonia were evident. The seizures initially responded to clonazepam, but, after the age of 5 mo, antiepileptic drugs could no longer control them. With time, the seizures evolved into tonic seizures, and, after the age of 7 years, dyskinesias with short choreatiform or myocloniclike movements also occurred. The frequency of seizures diminished in the following years, but the patient made no developmental progress. The patient had dysmorphic features, with hypertelorism, high nasal bridge, large but narrow and not well-modeled ears, a low posterior hairline, and a simian crease (fig. 1). Eye movements were uncoordinated, and there was no fixation to light or movement. The fundi were pale, with fine pigmentation. Cranial magnetic resonance imaging (MRI) at age 6 years showed ventricular enlargement and hypoplasia of the corpus callosum, cerebellum, and white matter. There was a mild conduction defect (43 m/s) in the median nerve, but values were normal in the lower limbs. Urine amino acids and organic acids and plasma lactate and pyruvate were normal, and GM-1 and GM-2 gangliosidosis were excluded. At age 7 years and 4 mo, length was 126 cm (50th percentile), weight was 17.4 kg (<3rd percentile), and head circumference was 49 cm (3rd percentile). The patient died at the age of 17 years.

Patient 2 was the first child of unrelated Indonesian parents. She was born at 38 wk gestation—following a normal pregnancy, labor, and delivery—with Apgar scores of 7 at 1 min and 8 at 5 min, head circumference of 35 cm (50th percentile), and birth weight of 3,000 g (10th–50th percentile). She was considered to be a normal child until age 2 mo, when extensor spasms appeared. EEG showed hypsarrhythmia, and a diagnosis of infantile spasms was made. Results of cerebral computed tomography (CT) and MRI scans were normal. The child made no developmental progress following the onset of seizures. With time, the seizures evolved into tonic seizures (poorly controlled by antiepileptic drugs) that persisted until her death at 3 years of age. Head circumference at 14 mo was 46 cm (50th percentile). Investigations of the following gave normal results: urine levels of amino acids, organic acids, mucopolysaccharides, and sulfite; cerebrospinal fluid levels of lactate, glycine, glucose, and protein; leukocyte lysosomal enzymes; plasma very-long-chain fatty acids; whole blood; thyroid function; and visual evoked potentials, electroretinogram, and brain stem auditory evoked responses.

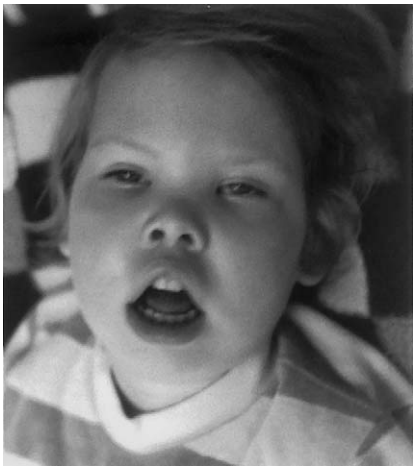

Figure 1 Patient 1 at the age of 3 years.

A clinical summary of both patients, in comparison with the features of patients with *ARX* mutations, as well as infantile spasms syndrome/WS, is presented in table 1.

Cytogenetic Investigations and Cosmid Library Screening

Samples from patients and parents were obtained after informed consent. Chromosome analysis was performed using standard high-resolution techniques (Dutrillaux 1981).

Initial FISH experiments were performed with YAC clones from the region of interest. Fine mapping of breakpoints was performed with smaller BAC/PAC and cosmid clones. DNA samples were prepared according to standard protocols and were labeled with either biotin-16-dUTP or digoxigenin-11-dUTP, by Nick trans-

Table 1

Clinical Summary of Patients 1 and 2 with Disrupted *STK9* Genes, Compared with the Features of Patients with *ARX* Mutations and Patients with Infantile Spasms Syndrome/WS

Feature	Patient 1	Patient 2	*ARX* Disorders	Infantile Spasms Syndrome/WS
Sex	Female	Female	Males	Males and females
Mental retardation; severity	Yes; profound	Yes; profound	All; 58% mild-moderate, 42% severe to profound	Most (70%–90%); severe to profound
Seizures	Yes	Yes	58%	All
Presenting seizure type	Infantile spasms	Infantile spasms	Infantile spasms (59% generalized tonic-clonic, 34% absence, 3.5% unspecified)	Infantile spasms
Age at onset	3 mo	2 mo	Varies by mutation	<1 year (usually 3–8 mo)
EEG results	Hypsarrhythmia	Hypsarrhythmia	Hypsarrhythmia in most	Hypsarrhythmia in most
Subsequent seizure type	Tonic	Tonic	Generalized tonic-clonic, absence, myoclonic, atonic, and complex partial seizures	30%–50% have another seizure type (partial, myoclonic, tonic, or tonic-clonic)
Other neurological features	Dyskinesias with choreiform and myoclonic movements, pale fundi with fine pigmentation	None	Dystonia/Partington syndrome, autism, and spinocerebellar ataxia	Depends on etiology (e.g., cerebral palsy)
Nonneurological features	Mildly dysmorphic facial features, head circumference 3rd percentile	Head circumference 50th percentile	Macrocephaly and microcephaly	Depends on etiology
Familial occurrence	No	No	Common	Uncommon
Etiology	*STK9* mutation	*STK9* mutation	*ARX* mutation	Heterogeneous

lation. Immunocytochemical detection of probes was performed exactly as described elsewhere (Wirth et al. 1999). Chromosomes were counterstained with 4′6-diamino-2-phenyl-indole (DAPI). Metaphases were analyzed with a Zeiss epifluorescence microscope.

The spotted Lawrence Livermore X-chromosome–specific cosmid library was hybridized with a pool of PCR products of the candidate region. Fragments were labeled with α^{32}[P]dCTP by random priming. Labeled probes were preannealed with Cot1 DNA (Gibco) for 1 h at 65°C, and they were then hybridized overnight at the same temperature, washed, and photographed using Kodak X-Omat AR film.

Molecular Investigations

For Southern blot analysis, genomic DNA from the patients and control DNAs were digested using *Bam*HI, *Eco*RI, *Hin*dIII, and *Eco*RV and were size-separated in 0.7% agarose gels. The DNAs were blotted onto nylon membranes and were hybridized with α^{32}[P]dCTP-labeled random hexamer primed PCR products. For patient 1, the breakpoint-spanning probe for Southern blot hybridization was generated using the following PCR primer set: STK9_F (5′-GTATTTGAAGCCTCCCATCG-3′) and STK9_R (5′-CTAAACTGGCAGAAGCACAGG-3′), (positions 76261–77382 of clone 245G19; GenBank accession number Z92542). For patient 2, the 1-kb probe for Southern blot hybridization was generated from genomic DNA (positions 19–930 of the 958B3 clone; GenBank accession number Z93023), using the following PCR primers: 958B3-F (5′-GGATCGGGTTTCCAAGGAGGAT-3′) and 985B3-R (5′-ACTAAACTGCAAGTGACTGCAAG-3′), resulting in a 912-bp amplicon.

Adaptor-ligated PCR was performed as described by Siebert et al. (1995), using *Eco*RI-digested patient DNA and a nested set of primers. Primer sequences are available, on request, from the authors. Amplified fragments were isolated on 1% agarose gels and were purified with Qiagen columns and sequenced.

Total RNA was isolated from fetal brain, fibroblast, and lymphoblastoid cell lines, using Trizol (Gibco); testis RNA was purchased from Clontech. RT was performed with random hexanucleotide primers and Superscript II (Gibco). In each experiment, DNA contamination was excluded by amplifying samples in parallel without the addition of RT. For patient 1, *STK9* expression was analyzed with the following primer sets: 5BP-F (5′-TGAAAGTTCCCACCAACCAG-3′) (located in exon 2) and 5BP-R (5′-AAGTAAGAGTTCTGGGGACC-3′) (located

Table 2

Primer Sequences and Conditions for the PCR Amplification of the *STK9* Exons from Genomic DNA

Exon	Forward Primer	Reverse Primer	Product Size (bp)	Optimal Conditions	
				Mg^{2+}	Temperature (°C)
1	CTCTCC AGC CCA GGT TGC TAG	GGT CTC CAC TCT CAG GAG AAG C	506	1.5	60
2	TAA GAT TGG TAC TAG AGT ACT GC	GAC ACA CAT GTG AAT TGA TAT AGG	412	1.5	60
3	GAG AAG CAA TGT CAG TAT AGC AG	CAT GCC CAC ACG CAA AGA CCA C	194	1.5	60
4	CAA CTG GAA TCC CCA GTC GGA	AGT GTC TGA CCA GCT AGA TCC	222	.5	60
5	GAA GTA CTC AAA GCA GAA GGT GA	TCG GGC AAA TGT GCA CAT TGG C	285	.5	60
6	GCT CTG TAT TGG ATG AAT TAT TCT AG	GAC AGT AAC ATG TGA AAT ACT CTT AAC	297	1.5	55
7	CAG TGT CAA TCA GGA GAA CAT AG	TAA TTC TGT AAG TAC CAG GAC TTA	163	1.5	55
8	GCC CAT GCG AGA ACA GTC ATT AC	GCA AAT GAC AAT AGA ATC AGC AG	280	1.5	55
9	AGT TGC CAA AAT AAT CTC TTC CTT	GAA CAA TGA CTC AAA TAC TGC AG	284	1.5	55
10	AAC ACT CAC AAG CAC GTG CA	TTA TTT GCC ATT CCA CAT CTC CT	273	1.5	55
11	GAC TTT GTA ATG TTC TTA ACG ATC	CTA ATT GCA TCA TTT AAG CAG CC	281	1.0	60
12	TTG TGT GTC AGC TAT TGA GGG	GGT ATG TTG TTG TTG GTG AGA TC	284	1.5	55
12a	TGC ACA CCA AAA CCT ACC AAG C	GCT TTT GGC CTT GGT CCT GTA GGA	329	1.5	55
12b	GAG TCG GCA TAG CTA TAT TGA CAC	GAA TGG CTA CTG TCC ATG TGC	354	1.5	55
12c	AAC GCT GGA CTC ACG TCG AAC	CCA CCA GAT TCA GTC AAG GTG	318	1.5	55
13	CTG GTT ATG GTC CTA GTT CTA CC	GTG GGA GAC TGG GTA TTA ATA C	285	1.5	55
14	CAT AGG CAA TAT TGT CAT CAA TGT G	GTG TAG GTG AGA AGG CCG CTG	269	2.0	60
15	GAA AAG TCC ATC AGT GAC TTA C	GGA CAC TAA AAA GCT CAT CCA GA	249	1.5	55
16	GGC TAT AGG AAC CTA GTG TCA TG	AAG TGC AAA GTG TAA AGT ATC CAT	282	1.5	55
17	CTC CTC TTG GGT GTG GTT GC	GCT CAG CCT TAC TGT AAC ATT G	312	1.0	60
18	TCT AAC TTG AAT CCT GTG TGC	TCC TGG TCA CAG AGG ACA CAT G	301	.5	58
19	GTG GGC AGA AGT GGC CAA TA	GTC TAG GGT CGT TAT GGC AGC	223	1.0	58
20	ACC TTG GCT TCA GCT GGT GTC	GGG CAA TTC CGA GGT ACA GC	325	2.0	60
21	GCC AGA GTG CAC CTG CTA GC	AAG GAA AAC TCA ACC TCA GCG	286	1.0	58

in exon 8), with an amplicon of 678 bp; BPf 5′-TGGGCTGTATTCTTGGGGA-3′ (located in exon 9) and BPr 5′- TTCTCGTGTCACTGTGTCTG-3′ (located in exon 12), with an amplicon of 1,029 bp; 3BPf 5′-GTCAAAGAGACCTCCAGAGA-3′ (located in exon 13) and 3BPr 5′-GGGGTGAATCCGAATTTCTG-3′ (located in exon 18), with an amplicon of 645 bp.

For patient 2 the following *STK9* gene-specific primers, flanking the ATG translation start site, were used; STK9.1 5′-GTTCCCACCAACCAGTGAGAA-3′ (located in exon 2), and STK9.2 5′-TTTAAGTACAACTCCATAGGCTC-3′ (located in exon 3). The STK9.1/STK9.2 primers amplify a 208-bp amplicon only from cDNA. As a control of the integrity of the isolated RNA, esterase D (*ESD*)–specific primers were used, as described elsewhere (Gécz et al. 1997).

Expression of *STK9* isoform II–containing exons 1a and 1b was investigated with primer set STK9.1a 5′-AGACCCTACAGGAAGTTGAG-3′ (located in exon 1a) and 5BPr (located in exon 8; see above), followed by seminested amplification with primers STK9.1a and STK9.ex8 5′-CCATCTGGTGGCACGTAC-3′ (located in exon 8).

For patient 1, *ARX* expression was analyzed with the following primer set: (ARXcF2 5′-CGCTCGACTCCGCTTGGACTG-3′) and ARX0-5R (5′-GAGTGGTGCTGAGTGAGGTGA-3′), followed by seminested PCR with ARXcF2 and ARXcE5STOPR 5′-GCAGCCTTTAGCACACCTCCT-3′. Amplification was performed in the presence of DMSO. *STK9* mutation screening has been performed using the intronic primers and PCR conditions listed in table 2. *ARX* gene mutation screening has been performed by SSCP (primers are available upon request from J.G.).

Results

Karyotypes

Patient 1 carried a balanced translocation between the distal short arm of chromosome X and the distal short arm of chromosome 7. Her karyotype was 46,X,t(X;7)(p22.3;p15). The ideogram is depicted in figure 2*A*. Patient 2 carried a balanced translocation between the distal short arm of chromosome X and the proximal short arm of chromosome 6. Her karyotype was 46,X,t(X;6)(p22.3;q14) (see fig. 2*B*). Neither translocation was detected in the parents; thus, both were considered as de novo translocations. The X-inactivation pattern was studied cytogenetically and molecularly for both patients. These experiments indicated 100% inactivation of the normal X chromosome (results not shown). For patient 2, complete skewing of the normal X chromosome was also further supported by the *STK9* RT-PCR experiments, which showed complete absence

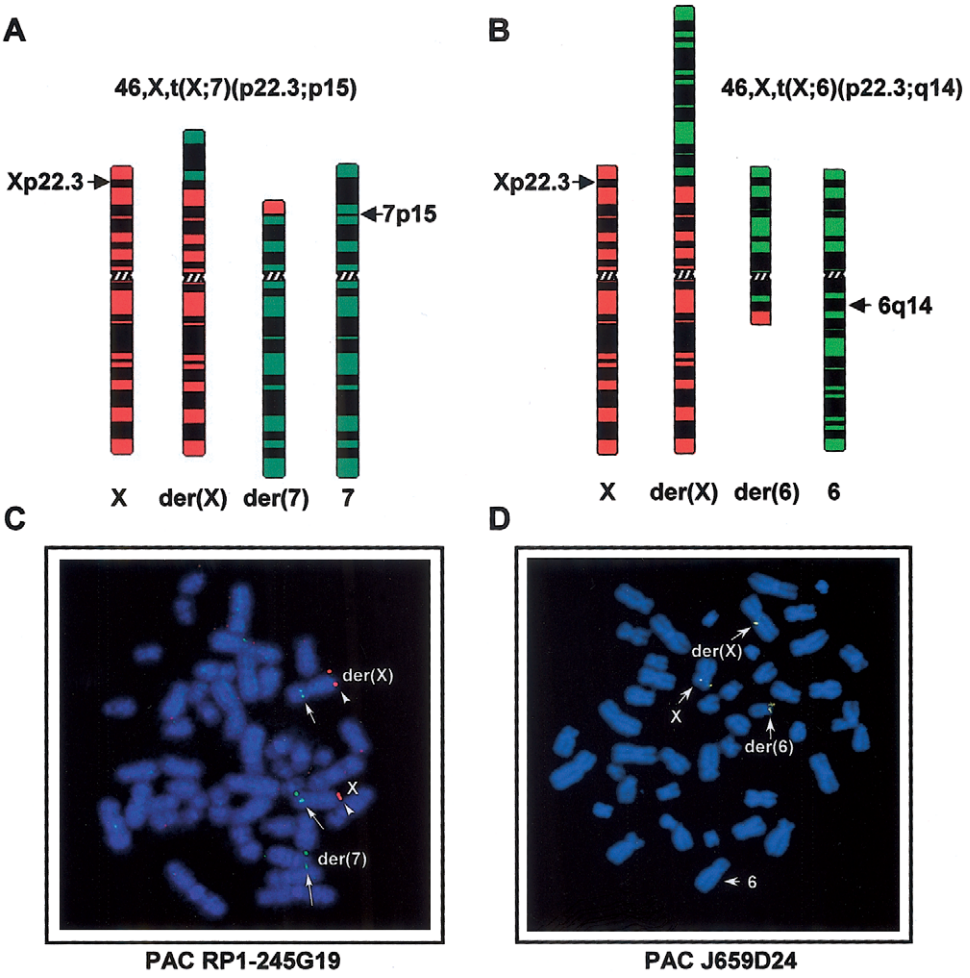

Figure 2 FISH mapping of the Xp22.3 translocation breakpoints. *A*, Ideograms of chromosomes X and 7 and their derivatives der(X) and der(7) in patient 1 with 46,X,t(X;7)(p22.3;p15), with indications of breakpoints (*arrows*). *B*, Ideograms of chromosomes X and 6 and their derivatives der(X) and der(6) in patient 2 with 46,X,t(X;6)(p22.3;q14). *C*, FISH analysis of the patient's chromosomes with the breakpoint-spanning clone RP1-245G19, which shows signals on the normal X chromosome, the der(X), and the der(7) (*arrows*). Cohybridization with an Xptel-specific cosmid probe was used to indicate the normal and derivative X chromosomes (*arrowheads*). Arrows point to the breakpoints. *D*, The metaphase shows the breakpoint-spanning PAC J659D24 with signals on the normal X chromosome and split signals on the very large derivative X and the derivative chromosome 6.

of the *STK9* transcript from lymphoblastoid RNA (see below and fig. 3*C*).

Cytogenetic Studies

Initially, breakpoints were investigated by FISH. The X chromosomal breakpoints were mapped with a set of cytogenetically and genetically anchored YACs, 18–26 cM, established at the Mendelian Cytogenetic Network (MCN) Reference Center. In patient 1, signals from the overlapping YAC 939h7 were found on both derivative chromosomes, whereas YAC 935f7 gave a signal only on der(7), and YAC 742h9 gave a signal only on der(X). In patient 2, hybridization signals of YAC 896f9 appeared only on the der(6), and YAC 960a5 showed signals only on the der(X). The results placed both X chromosomal breakpoints within the interval between markers DXS1195 and DXS999 (results not shown). Subsequent FISH with BAC and PAC clones from the DXS1195–DXS999 region further narrowed the positions of both translocation breakpoints. In patient 1, PAC RP1-245G19 (Z92542) showed split signals; in patient 2, the more distally located PAC J659D24 (Warneke-Wittstock et al. 1998) overlapped the breakpoint. The results are shown in figures. 2*C* and 2*D*. PAC RP1-245G19 contains all but exons 1, 1a, 1b, 2, and 3 of *STK9*, a pseudogene similar to α-1 protein, and the 3′ end of the *XLRS1* gene (X-linked juvenile retinoschisis precursor protein). In patient 1, further refinement of the breakpoint was achieved by FISH mapping the cosmid clones LANLc153A2441 and LANLc153P0827,

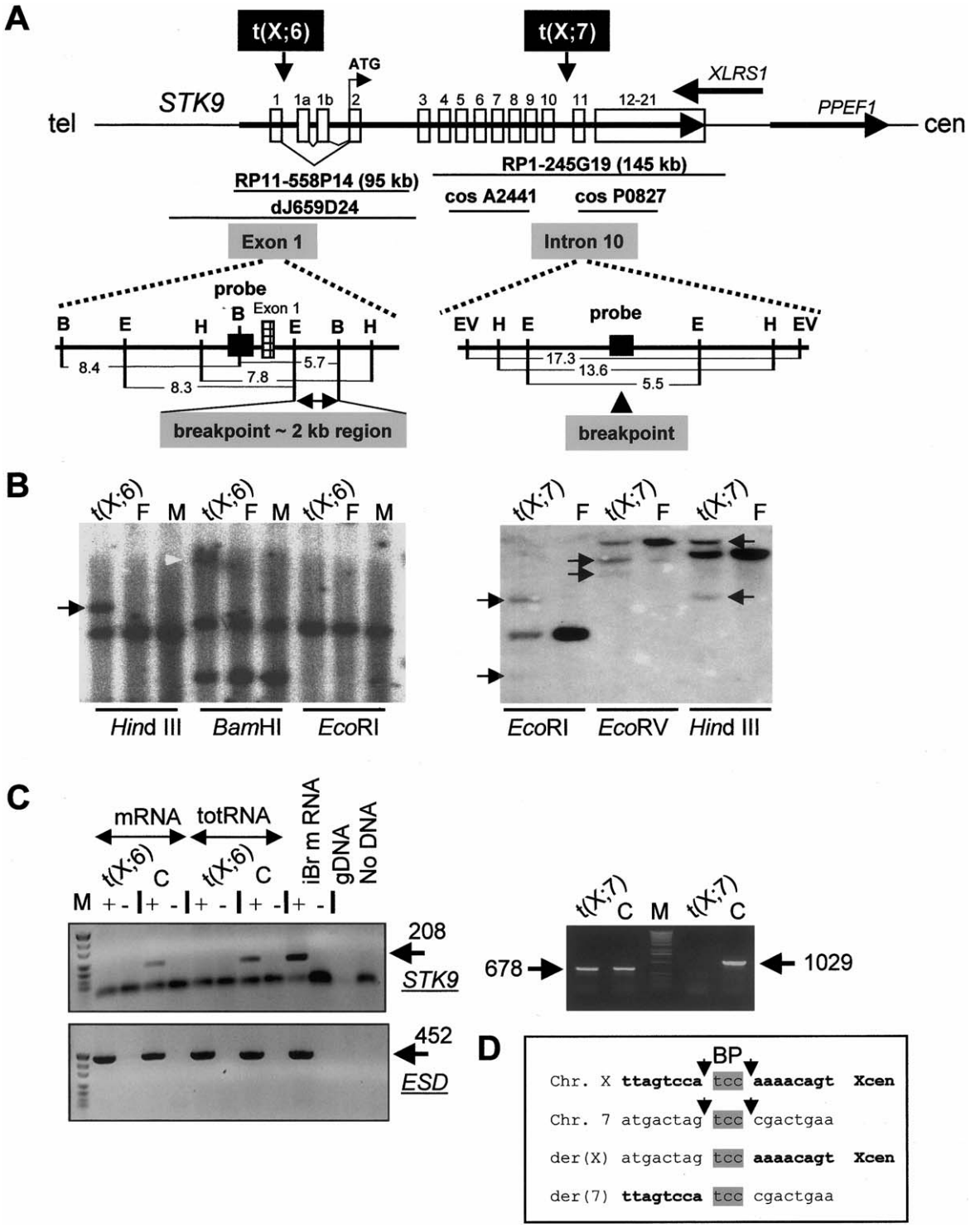
A
t(X;6)
t(X;7)
ATG
XLRS1
STK9
1 1a 1b 2 3 4 5 6 7 8 9 10 11 12-21
tel
PPEF1
cen
RP11-558P14 (95 kb)
RP1-245G19 (145 kb)
dJ659D24
cos A2441
cos P0827
Exon 1
Intron 10
probe
B E H B Exon 1 E B H
8.4
8.3
7.8
5.7
breakpoint ~ 2 kb region
EV H E probe E H EV
17.3
13.6
5.5
breakpoint
B
t(X;6) F M t(X;6) F M t(X;6) F M
Hind III BamHI EcoRI
t(X;7) F t(X;7) F t(X;7) F
EcoRI EcoRV Hind III
C
mRNA totRNA iBr m RNA gDNA No DNA
t(X;6) C t(X;6) C
M + - + - + - + - + - + -
208
STK9
452
ESD
t(X;7) C M t(X;7) C
678
1029
D
BP
Chr. X ttagtcca tcc aaaacagt Xcen
Chr. 7 atgactag tcc cgactgaa
der(X) atgactag tcc aaaacagt Xcen
der(7) ttagtcca tcc cgactgaa

which were positive in a screen with PCR products from the candidate region. Cosmid LANLc153A2441 showed signals on the der(7), and cosmid LANLc153P0827 showed signals on the der(X), thereby narrowing the breakpoint region to a small interval (results not shown).

The breakpoint on chromosome 7 was similarly characterized. YAC 743f9 (at 63–65 cM, with markers AFMA283XF5, D7S671, D7S691, D7S2548, WI-620, and D7S2746) hybridized strongly to der(7) and weakly to der(X), whereas YAC 776a4, which has at least the marker D7S691 in common, showed signals only on der(7), and YAC 956e1 (at 61 cM) gave signals only on der(X). We then narrowed the chromosome 7 breakpoint to the 600-kb interval between PAC RP5-953B5 (GenBank accession number AC004934) and BAC RP11-706L12 (GenBank accession number AC073852). We did not investigate the chromosome 6 breakpoint of patient 2.

STK9 *on Xp22.3 Is Truncated in Two Female Patients with X;Autosome Translocation*

In patient 1, Southern blot hybridization with a PCR product of clone RP1-245G19 detected two aberrant fragments in each digest but not in control DNA (fig. 3*B, right panel*), indicating that this probe is spanning the breakpoint. Cloning of the der(X) junction fragment was performed by ligation-mediated PCR on *Eco*RI-digested DNA. Sequencing of the specific PCR product and subsequent alignment with the *STK9* gene indicated that the breakpoint lies in intron 10, around position 77101 or 77104 of clone RP1-245G19 (fig. 3*D*).

In patient 2, we were able to map the X chromosomal breakpoint to within 2 kb of genomic sequence around exon 1 (this is the new *STK9* exon 1, not the exon 1 described by Montini et al. [1998]). The PCR-generated 1-kb probe from the end of the clone 958B3 (GenBank accession number Z93023) detected aberrant fragments on *Hind*III and *Bam*HI restriction digests but not on *Eco*RI digest (see fig. 3*B*, left panel). This localized the breakpoint to a maximum of 2.0 kb of the *Eco*RI-*Bam*HI fragment of intron 1 of *STK9*. The breakpoint was not further refined.

We have also revisited the complete gene structure of *STK9* by aligning entries from the database and our cDNA sequence (GenBank accession number AY217744) with genomic clones RP11-558P14 (GenBank accession number AL109798) and RP1-245G19 (GenBank accession number Z925542). We thereby found several discrepancies with the exon number and sizes given by Montini et al. (1998) (GenBank accession number Y15057). First, *STK9* is composed of 23 exons and not 20. The first three exons (1, 1a, and 1b) are untranslated and probably represent two transcription start sites of the *STK9* gene (see fig. 3*A, upper panel*) separated by ~17 kb. Exon 2 contains the ATG translation start codon, which is also conserved in mouse (J.T. and V.M.K., unpublished data). Second, exon sizes are as follows: exon 1 is 111 bp, exon 1a is 73 bp, exon 1b is 49 bp, exon 7 is 60 bp (as in Fugu genes [Brunner et al. 1999]), exon 17 is 120 bp, exon 18 is 217 bp, exon 20 is 183 bp, and exon 21 is 198 bp (see table 3).

The *STK9* RNA isoform containing exons 1a and 1b (isoform II) is transcribed at a very low level in human fetal brain and testis but not in lymphoblastoid cell lines (ESTs with GenBank accession numbers AL704691 and BI559845 and the mRNA with GenBank accession number BC036091) (results not shown). In contrast, *STK9* RNA containing exon 1 (isoform I) is expressed in a wide range of cells, including human fibroblasts and lymphoblastoid cell lines, which allowed us to study its expression in both patients. In patient 1, RT-PCR experiments with primers located in *STK9* exons 2 and 8 on der(7) resulted in a product of expected size, whereas no amplification product could be obtained with breakpoint-flanking primers located in exons 9 and 12 or with primers 3′ to the breakpoint, designed in

Figure 3 *A,* Diagram of the genomic structure of the *STK9* gene and selected clones used for breakpoint mapping by FISH. Exons (*unshaded boxes*) and introns are not drawn to scale. The respective positions of the two breakpoints studied, (t(X;7)(p22.3;p15) and t(X;6)(p22.3;q14), are indicated on top. The lower panel shows a restriction map of the area surrounding both breakpoints, with probes used for Southern blot hybridization indicated as solid rectangles. Position and size of the normal restriction fragments detected by the two probes is indicated (B = *Bam*HI, E = *Eco*RI, H = *Hin*dIII, EV = *Eco*RV). *B*, Southern blot analysis, using the probes indicated as solid rectangles in the lower panel of *A*. Patient DNA—with (tX;6) and t(X;7)—and control DNAs (F = female, M = male) were digested with the indicated enzymes. Rearranged (junction) fragments (*arrows*) are present only in the patients but not in the controls. *C*, RT-PCRs in patients' lymphoblastoid (tX;6) and fibroblast (tX;7) RNAs and control RNAs (C = control lymphoblastoid cell line RNA in case of t(X;6), C = control fibroblast RNA in case of t(X;7), iBr mRNA = infant brain mRNA, gDNA = genomic DNA, M = size marker). The left side of this panel shows a specific *STK9* amplification product of 208 bp (primers STK9.1 and STK9.2, see "Subjects and Methods" section) in all control RNAs but not in patient RNA. The low molecular weight band visible in almost all lanes represents the primer dimer product. The *esterase D* (*ESD*) gene served as a control for patient cDNA established from mRNA and total RNA. The right side shows specific RT-PCR products of 678 bp with a primer set spanning *STK9* exons 1–10 in both patient and control RNA. Primers spanning the breakpoint (located in exons 9 and 12) amplify *STK9* transcripts of 1,029 bp in the control but not in the patient. *D*, Chromosome X, 7, der(X) and der(7) sequences at the breakpoints in patient 1. Chromosome X–derived sequences are shown in bold. The breakpoints are on either side of the common 3-bp sequence (*shaded boxes*).

Table 3

Exon Numbers, Splice Junction Sequences, and Exon Sizes of the *STK9* Gene

Exon No.	3′ Splice Site	5′ Splice Site	Exon Size (bp)
1		ACTCGGCGGGgtgagtagtc	111
1a		GGAAGTTGAGgtatcatatc	73
1b	tggtgtccagCTGTACTCTC	CTCCCTTCAGgtactctcct	49
2	tttttttcagGGAGTCATTT	GTAGGTGAAGgtaagttgga	126
3	tttattatagGAGCCTATGG	CAGACACAAGgcaagtacat	35
4	tcccttgcagGAAACACATG	GACAGTGAAGgtagatatat	46
5	tacattctagAAAATGAAGA	TGTTGAAAAAgtaagtcatt	137
6	taatttttagAATATGCTCG	GTCCATCGAGgtgagtatga	121
7	gacactccagATATAAAACC	TGTGACTTTGgtaagttaaa	60
8	tatctttcagGTTTTGCTCG	TCTTACTTGGgtgagttacc	91
9	tatttttcagCGCTCCCTAT	TGGGCTCCGGgtaagaggtt	190
10	tgtctcacagTTTCCAGCTG	CCTAATGAAGgtaaggccaa	81
11	atttcctaagAATTTACTGA	TGTCTAATAGgtaaatattc	152
12	tttaacatagAAACCAAGCC	GTCACCCCAGgtacagttga	967
13	ttacttccagCCTGGAGAAC	GAAGTCTGAGgtatgtcaca	102
14	cctgcctcagGGTGGACTGT	TTTTACAGAGgtaagcccac	106
15	ctttattcagTGCCATCTCC	TCGATCCATGgtgagcattt	124
16	tctcatttagGAAAAGTCCT	ATCTCAAACAgtaagtagat	100
17	tttgctctagGTACCCAATT	GCAGACCCAAgtgagtggat	120
18	tttctttcagAGCCAGCCAT	CAGCTGCCAGgtcagatgga	217
19	caccaactagACGGTGGATG	GAACAACAAGgtagagtctg	84
20	tattttccagGAGAATACTT	CAGCAATCCGgtaagcagag	183
21	tgctttccagGGTTCTCTTT		198

NOTE.—Lowercase letters indicate intron sequence; uppercase letters indicate exon sequence; and underlining indicates consensus dinucleotides.

exons 13–18 on der(X) (fig. 3*C*, *right panel*). These results clearly indicate that *STK9* exons 1–10 are transcribed in patient 1. The truncated RNA would encode a protein of 275 amino acids, which may retain some functional properties.

In patient 2, the breakpoint has been located between exons 1 and 1a (figs. 3*A* and 3*B*). RT-PCR experiments with exon 2 and 3 primers failed to detect any *STK9* RNA. This was also true for another set of 3′ end–specific *STK9* RT-PCR primers (fig. 3*C* and results not shown). As a result, this patient does not express any detectable *STK9* RNA of the isoform I (originating from exon 1). Expression of the *STK9* isoform II (originating from exon 1a) could not be tested, because this isoform is not expressed in lymphoblasts. Precise position of the chromosome 6 breakpoint was not determined.

STK9 and *ARX* are separated by ~5 Mb of genomic sequence, as estimated from the Ensembl Human Genome assembly (*STK9* being at postion ~18.4 Mb and *ARX* at position ~23.8 Mb). In patient 1, *ARX* expression was identical to that of control fibroblasts (data not shown); therefore, a position effect is unlikely. The *ARX* gene is not transcribed in lymphoblastoid cell lines; thus, the analysis could not be performed in patient 2. SSCP screening of DNA of patient 2 for the *ARX* gene yielded no mutations.

In patient 1, we have also identified the chromosome 7 breakpoint by using adaptor-ligated PCR. It lies between exons 4 and 5 of the formerly predicted gene LOC168637. However, using several primer sets in RT-PCR, we could not amplify any predicted exon on fetal brain RNA, suggesting that this gene is either not expressed in brain or is not real. The latter possibility is further supported by negative BLAST searches of LOC168637 against ESTs in public databases. More recently, the gene prediction of LOC168637 has been removed from the database. Therefore, it is very unlikely that a gene on chromosome 7 is interrupted by the breakpoint.

To date, only a few studies describe short sequence motifs involved in human balanced chromosomal rearrangements (Giacalone and Franke 1992; Nothwang et al. 2000; Bonaglia et al. 2001). Analysis of the junction fragments in patient 1 revealed that the translocation is balanced with loss of a 3-bp sequence that is a common motif at the rearrangement sites of chromosomes X and 7 (fig. 3*D*).

STK9 Screening in Families with X-Linked WS/ISSX

Prior to the identification of the *ARX* gene as the major cause of the X-linked WS/ISSX (Strømme et al. 2002*b*), we used SSCP and direct sequencing to screen the *STK9* gene in the four previously published families

with ISSX (one reported by Strømme et al. [1999], two reported by Claes et al. [1997], and one reported by Bruyere et al. [1999]) and the family with XMESID (X-linked myoclonic epilepsy with spasticity and intellectual disability) reported by Scheffer et al. (2002). Furthermore, no disease-causing mutations were identified in the family B reported by Claes et al. (1997), which was also negative when screened for mutations in the *ARX* gene. We have detected only one cSNP, at position 2593 (2593A→C, exon 16), which results in the amino acid change Q791P. This cSNP was detected on 20% of a panel of 50 control chromosomes on which it was tested (results not shown).

Discussion

Disease-associated balanced chromosome rearrangements form a visible bridge between genotype and phenotype and have been instrumental in the identification of numerous disease genes. In the present study, we have characterized two female patients, one with a 46,X,t(X;7)(p22.3;p15) and the other with a 46,X,t(X;6)(p22.3;q14) apparently balanced translocation. The patients presented with a seemingly identical phenotype, comprising early-onset severe infantile spasms with profound global developmental arrest and hypsarrhythmia on the EEG. In patient 1, cranial MRIs in early childhood were normal, but she showed ventricular enlargement and hypoplasia of the corpus callosum, cerebellum, and white matter at age 6 years. Patient 2 died at age 3 years; results of cranial CT and MRI were normal. Such diagnoses as Aicardi syndrome (a rare, congenital X-linked disorder with the classic features of infantile spasms, callosal agenesis, and pathognomonic chorioretinal lacuna) and ISSX or X-linked WS were considered.

Cytogenetic investigations showed skewed X inactivation in both patients, which was later confirmed by molecular studies. The X chromosomal rearrangements disrupt *STK9* in both patients. In particular, the breakpoint in patient 2 is in the most 5′ end of *STK9,* and the major transcript is completely lacking, which further suggests that in normal female somatic cells *STK9* is subject to X-inactivation.

The truncation of *STK9* in these patients, together with normal *ARX* expression and the absence of the *ARX* gene mutations, strongly suggests that, in these patients, the disease was caused by either complete (patient 2, isoform I) or partial (patient 1, isoforms I and II) loss of STK9 protein function. Although in patient 1 either of the two isoforms is affected (truncated) by the translocation, in patient 2 it would be at least isoform I (containing exon 1) that is completely missing. The expression of the isoform II, which is likely to be transcribed from a different *STK9* promoter ~12 kb proximal to the breakpoint of patient 2, could not be tested, because this isoform is not transcribed in lymphoblasts (the only cell line available from patient 2). Position effect of the translocation on the promoter of *STK9* isoform II can also be considered. In the absence of data on *STK9* isoform II expression in patient 2, we can only speculate about the biological significance of this isoform. However, on the basis of the much lower expression level of isoform II and the different expression pattern of both *STK9* isoforms, it is highly unlikely that isoform II (if expressed in patient 2) would have been able to compensate for the lack of the major *STK9* isoform I.

The autosomal breakpoints most likely do not contribute to the phenotype, because they are on different chromosomes. In patient 1, the chromosome 7 breakpoint does not directly disrupt an obvious gene and lies distal to the 3′ end of *GLI3* (the gene mutated in Greig cephalopolysyndactyly syndrome [MIM 165240]) and proximal to the 3′ end of *INHBA* (MIM 147290), which may play a role in craniofacial development. The autosomal breakpoint in patient 2 has not been mapped in detail.

STK9 mutation analysis in all four published families with ISSX (one reported by Strømme et al. [1999], two reported by Claes et al. [1997], and one reported by Bruyere et al. [1999]) was negative, including the family B reported by Claes et al. (1997), which is the only *ARX*-negative family with ISSX (Strømme et al. 2002*b*). Taken together with our previous findings of *ARX* mutations causing ISSX (Bienvenu et al. 2002; Strømme et al. 2002*b*), these studies provide strong evidence that the etiology of ISSX is heterogeneous. Provided that the family B of Claes et al. (1997) does not have a mutation in either *STK9* (the present study) or *ARX* (Strømme et al. 2002*b*) genes, we may speculate the existence of yet another ISSX locus on Xp.

Additional circumstantial evidence implicating the *STK9* gene in epilepsy comes from the recent article by Huopaniemi et al. (2000). These authors performed a mutation search in Danish patients with retinoschisis and found a 136-kb deletion in two affected siblings with typical retinoschisis. The 3′ UTR region of *STK9* overlaps with the 3′ UTR of the *XLRS1* gene, which is the gene implicated in X-linked juvenile retinoschisis (XLRS). The rearrangement partly deleted *XLRS1* and also *PPEF-1* (protein phosphatase gene with EF calcium-binding domain) and truncated the 3′ end of *STK9,* including the last coding exon. One affected brother had epilepsy in addition to retinoschisis. It is unclear at present whether epilepsy in this case is related to the truncated *STK9* gene and whether other alterations in *STK9* can lead to a less severe form of ISSX.

STK9 was isolated in the course of a transcriptional mapping effort in the Xp22 region (Montini et al. 1998). Northern analysis revealed transcription in sev-

eral tissues, including fetal and adult brain. We have revised the genomic structure of the *STK9* gene. Several differences from the previous report by Montini et al. (1998) were detected. One of these differences is that the *STK9* gene contains at least 23 exons, the first three exons being untranslated and representing two *STK9* isoforms most likely transcribed from two different promoters (while both maintain the same ORF; see fig. 3*A*).

The predicted STK9 protein belongs to the large family of eukaryotic protein kinases that are related by the highly conserved kinase domain, which comprises 250–300 amino acids. Protein kinases have been involved very frequently in the pathogenesis of genetic disorders. At present we can speculate on STK9 function only by virtue of sequence comparison with known homologs. Its kinase domain is most closely related to human KKIAMRE and KKIARLE and their orthologs (Montini et al. 1998). These proteins are members of the mitogen-activated protein (MAP) kinase family that is related to cell-division cycle 2. MAP kinases are important regulators of synaptic plasticity in neurons. However, human KKIARLE is expressed in fibrous astrocytes in the white matter, in perivascular and subpial spaces, and in Bergmann glia in the cerebellum but not in neurons (Yen et al. 1995). In contrast, its mouse and rat counterparts are expressed in neurons in various brain regions, including the cerebral cortex and hippocampus, as evidenced by immunohistochemistry (Gomi et al. 1999; Sassa et al. 2000). KKIAMRE very likely plays a role in learning and memory and has been shown to be phosphorylated by MEK1, a protein kinase that activates MAP kinases in vitro (Taglienti et al. 1996; Gomi et al. 1999). These results suggest that STK9 protein may play a role in the MAP kinase cascade, although experimental evidence is needed to prove this hypothesis. In addition to this, BLAST searches revealed 44% identity and 64% similarity to cell division protein kinase 5 (τ protein kinase II catalytic subunit) and 43% identity and 63% similarity to cell division protein kinase 2 (p33 protein kinase). At present, we do not know the significance of the similarities between STK9 and other kinases. Identification of substrates for STK9 will help to determine the importance of these similarities.

Taken together, our observations indicate that *STK9* is a new ISSX locus and is the second gene implicated in infantile spasms, suggesting that the etiology of ISSX is heterogeneous. The overall contribution of *STK9* mutations in ISSX remains to be determined. Ongoing studies will shed more light on the role of STK9 and its substrate(s) and signaling pathway in the brain and will help to unravel the pathogenic mechanisms of ISSX.

Acknowledgments

We sincerely thank the members of the families and their clinicians, for participation in this study; C. Derwas and H. Madle, for help with cell culture; T. Fullston, for technical assistance; and B. Franco, for Xp YAC clones. This work was supported by the National Health and Medical Research Council of Australia, Deutsches Humangenom-Programm grant 01KW99087, and Nationales Genomforschungsnetzwerk grant 01GR0105.

Electronic-Database Information

Accession numbers and URLs for data presented herein are as follows:

BLAST, http://www.ncbi.nlm.nih.gov/BLAST/
Ensembl Genome Browser, http://www.ensembl.org/
GenBank, http://www.ncbi.nlm.nih.gov/Genbank/ (for *STK9* mRNA sequences [accession numbers AY217744, Y15057, BC010966, BC036091, BF679133, AL704691, and BI559845] and *STK9* genomic sequences [accession numbers AL109798, Z925542, and Z93023])
Mendelian Cytogenetic Network (MCN) Reference Center at the Max-Planck-Institute for Molecular Genetics, http://www.molgen.mpg.de/~cytogen/
Online Mendelian Inheritance in Man (OMIM), http://www.ncbi.nlm.nih.gov/Omim/ (for ISSX, GLI3, and *INHBA*)

References

Bienvenu T, Poirier K, Friocourt G, Bahi N, Beaumont D, Fauchereau F, Ben Jeema L, Zemni R, Vinet MC, Francis F, Couvert P, Gomot M, Moraine C, van Bokhoven H, Kalscheuer V, Frints S, Gécz J, Ohzaki K, Chaabouni H, Fryns JP, Desportes V, Beldjord C, Chelly J (2002) *ARX*, a novel Prd-class-homeobox gene highly expressed in the telencephalon, is mutated in X-linked mental retardation. Hum Mol Genet 11:981–991

Bonaglia MC, Giorda R, Borgatti R, Felisari G, Gagliardi C, Selicorni A, Zuffardi O (2001) Disruption of the *ProSAP2* gene in a t(12;22)(q24.1;q13.3) is associated with the 22q13.3 deletion syndrome. Am J Hum Genet 69:261–268

Brunner B, Todt T, Lenzner S, Stout K, Schulz U, Ropers HH, Kalscheuer VM (1999) Genomic structure and comparative analysis of nine Fugu genes: conservation of synteny with human chromosome Xp22.2-p22.1. Genome Res 9:437–448

Bruyere H, Lewis, SE, Wood S, MacLeod PJ, Langlois S (1999) Confirmation of linkage in X-linked infantile spasms (West syndrome) and refinement of the disease locus to Xp21.3-Xp22.1. Clin Genet 55:173–182

Claes S, Devriendt K, Lagae L, Ceulemans C, Dom L, Casaer P, Raeymaekers P, Cassiman JJ, Fryns JP (1997) The X-linked infantile spasms syndrome (MIM 308350) maps to Xp11.4-Xpter in two pedigrees. Ann Neurol 42:360–364

Dutrillaux B, Viegas-Pequignot E (1981) High resolution R- and G-banding on the same preparation. Hum Genet 57: 93–95

Gécz J, Bielby S, Sutherland GR, Mulley JC (1997) Gene structure and subcellular localization of FMR2, a member of a new family of putative transcription activators. Genomics 44:201–213

Giacalone JP, Francke U (1992) Common sequence motifs at the rearrangement sites of a constitutional X/autosome

translocation and associated deletion. Am J Hum Genet 50: 725–741

Gomi H, Sun W, Finch CE, Itohara S, Yoshimi K, Thompson RF (1999) Learning induces a Cdc2-related protein kinase, KKIAMRE. J Neurosci 19:9530–9537

Huopaniemi L, Tyynismaa H, Rantala A, Rosenberg T, Alitalo T (2000) Characterization of two unusual *RS1* gene deletions segregating in Danish retinoschisis families. Hum Mutat 16:307–314

Kitamura K, Yanazawa M, Sugiyama N, Miura H, Iizuka-Kogo A, Kusaka M, Omichi K, Suzuki R, Kato-Fukui Y, Kamiirisa K, Matsuo M, Kamijo S, Kasahara M, Yoshioka H, Ogata T, Fukuda T, Kondo I, Kato M, Dobyns WB, Yokoyama M, Morohashi K (2002) Mutation of *ARX* causes abnormal development of forebrain and testes in mice and X-linked lissencephaly with abnormal genitalia in humans. Nat Genet 32:359–369

Montini E, Andolfi G, Caruso A, Buchner G, Walpole SM, Mariani M, Consalez G, Trump D, Ballabio A, Franco B (1998) Identification and characterization of a novel serine-threonine kinase gene from the Xp22 region. Genomics 51: 427–433

Nothwang HG, Schroer A, van der Maarel S, Kübart S, Schneider S, Riesselmann L, Menzel C, Hinzmann B, Vogt D, Rosenthal A, Fryns J, Tommerup N, Haaf T, Ropers HH, Wirth J (2000) Molecular cloning of Xp11 breakpoints in two unrelated mentally retarded females with X;autosome translocations. Cytogenet Cell Genet 90:126–133

Sassa T, Gomi H, Sun W, Ikeda T, Thompson RF, Itohara S (2000) Identification of variants and dual promoters of murine serine/threonine kinase KKIAMRE. J Neurochem 74: 1809–1819

Scheffer IE, Wallace RH, Phillips FL, Hewson P, Reardon K, Parasivam G, Strømme P, Berkovic SF, Gécz J, Mulley JC (2002) X-linked myoclonic epilepsy with spasticity and intellectual disability: mutation in the homeobox gene *ARX*. Neurology 59:348–356

Siebert PD, Chenchik A, Kellogg DE, Lukyanov KA, Lukyanov SA (1995) An improved PCR method for walking in uncloned genomic DNA. Nucleic Acids Res 23:1087–1088

Strømme P, Mangelsdorf ME, Scheffer I, Gécz J (2002*a*) Infantile spasms, dystonia, and other X-linked phenotypes caused by mutations in Aristaless related homeobox gene, *ARX*. Brain Dev 24:266–268

Strømme P, Mangelsdorf ME, Shaw MA, Lower KM, Lewis SME, Bruyere H, Lütcherath V, Gedeon AK, Wallace RH, Scheffer IE, Turner G, Partington M, Frints SGM, Fryns JP, Sutherland GR, Mulley JC, Gécz J (2002*b*) Mutations in the human ortholog of Aristaless cause X-linked mental retardation and epilepsy. Nat Genet 30:441–445

Strømme P, Sundet K, Mork C, Cassiman JJ, Fryns JP, Claes S (1999) X linked mental retardation and infantile spasms in a family: new clinical data and linkage to Xp11.4-Xp22.11. J Med Genet 36:374–378

Taglienti CA, Wysk M, Davis RJ (1996) Molecular cloning of the epidermal growth factor–stimulated protein kinase p56 KKIAMRE. Oncogene 13:2563–2574

Warneke-Wittstock R, Marquardt A, Gehrig A, Sauer CG, Gessler M, Weber BH (1998) Transcript map of a 900-kb genomic region in Xp22.1-p22.2: identification of 12 novel genes. Genomics 51:59–67

Wirth J, Nothwang HG, vander Maarel S, Menzel C, Borck G, Lopez-Pajares L, Brondum-Nielsen K, Tommerup N, Bugge M, Ropers HH, Haaf T (1999) Systematic characterization of disease associated balanced chromosome rearrangements by FISH: cytogenetically and genetically anchored YACs identify microdeletions and candidate regions for mental retardation genes. J Med Genet 36:271–278

Wong M, Trevathan E (2001) Infantile spasms. Pediatr Neurol 24:89–98

Yen SH, Kenessey A, Lee SC, Dickson DW (1995) The distribution and biochemical properties of a Cdc2-related kinase, KKIALRE, in normal and Alzheimer brains. J Neurochem 65:2577–2584